Long Range Metal-Metal Interactions Along Fe−NC−Ru−CN−Fe Chains

Tianlu Sheng[a] and Heinrich Vahrenkamp*[a]

Keywords: Chain structures / Cyanide complexes / Polynuclear complexes / Metal−metal interactions

Trinuclear complexes with linear Fe^{II}–NC–Ru^{II}–CN–Fe^{II} arrays were obtained by attachment of FeCp(dppe) units to the cyanoruthenium complexes *trans*-[$Ru(CN)_2(Py)_4$] (Py = pyridine, 4-methylpyridine, 4-ethylpyridine) . From their cyclic voltammograms it can be concluded that there are long-range metal–metal interactions between their external iron centers. Partial oxidation led to the isolation of the corresponding mixed-valent Fe^{II}–NC–Ru^{II}–CN–Fe^{III} complexes. For these the long range metal–metal interactions are evident from a broad MMCT band in the NIR spectra. The MMCT properties were quantified by an analysis using the Hush formalism.

Introduction

Cyanide-linked coordination polymers have attractive optical, electrical and magnetic properties.[1−3] The basis of these are metal−metal interactions across the bridging cyanide ligands. For this reason numerous studies have been undertaken on cyanide-bridged low-molecular complexes, with the purpose of elucidating the molecular equivalents of the bulk properties in terms of electron transfer, metal−metal charge transfer and molecular magnetism.[4]

The simplest objects of study in this respect would be chain-like complexes with linear arrays of metals and bridging cyanide ligands. It turns out, however, that long chains of this kind are difficult to synthesize, and until today no such complex with more than three metal atoms has been unambiguously identified in solution or obtained analytically pure. Moreover, proof of long-range metal−metal interactions in trinuclear complexes with M−CN−M′−CN−M arrays, for instance by the typical splitting of the cyclovoltammetric redox waves, has been achieved in only a rather small number of cases.[5,6−8]

Our own investigations in the area of chain-like cyanide-bridged trinuclear complexes have virtually doubled the number of species for which evidence of remote metal−metal interactions exists.[9−14] For the first time we could also subject a group of such complexes to preparative one-electron oxidations and isolate mixed-valent trinuclear complexes with Fe^{II}-(μ-CN)-Pt^{II}-(μ-CN)-Fe^{III} arrays.[9] Yet, despite a wide variation of the building blocks, the supporting ligands, the oxidation states of the metals and the shape of the M−CN−M′−CN−M chains we have not yet found conclusive evidence as to which factors govern the occurrence and the extent of their remote metal−metal interactions.

The present study contributes one such piece of evidence. The complexes under investigation have *trans*-[$Ru^{II}(CN)_2Py_4$] units at the center and FeCp(dppe) units at the external positions which turned out to be favorable for redox reactions and spectroscopic measurements. $RuPy_4(CN)_2$-centered complexes with external $Ru(NH_3)_5$ [7] and $Ru(Py)_4Cl$ units[15] have already been described and subjected to electrochemical and spectroscopic measurements as well as a theoretical treatment of vibronic coupling in them.

Results and Discussion

Preparations and Structures

Previously we have investigated L_nM-(μ-CN)-$M'^{II}(Py)_4$-(μ-CN)-ML_n complexes with M'^{II} ions from the first row of the transition metals at the center.[16] Their octahedral $M'X_2Py_4$ cores are labile, and hence $M'(NC)_2Py_4$ arrangements in the trinuclear complexes could not be prevented, even when starting from $M'(CN)_2Py_4$ complexes (cyanide-isocyanide rearrangement). In contrast, octahedral Ru^{II} complexes are quite inert, and it could be anticipated that the *trans*-[$Ru(CN)_2Py_4$] array would be maintained after the attachment of two organometallic L_nM units. This was expected to be favorable in two respects: first, the attachment of the cyanide's carbon terminus (the π-acceptor orientation of CN^-) to ruthenium should raise the Ru^{II}/Ru^{III} redox potential, and second the attachment of the nitrogen terminus (the σ-donor orientation of CN^-) to the L_nM unit should lower the redox potential of the latter. Hence it would be likely that a partially oxidized (i.e. mixed-valent) species would have the oxidation state M^{II}−NC−Ru^{II}−CN−M^{III}, and that electronic communication between M^{II} and M^{III}

[a] Institut für Anorganische und Analytische Chemie der Universität Freiburg,
Albertstr. 21, 79104 Freiburg, Germany
Fax: (internat.) + 49-(0)761-203-6001
E-mail: vahrenka@uni-freiburg.de

  DOI: 10.1002/ejic.200300656

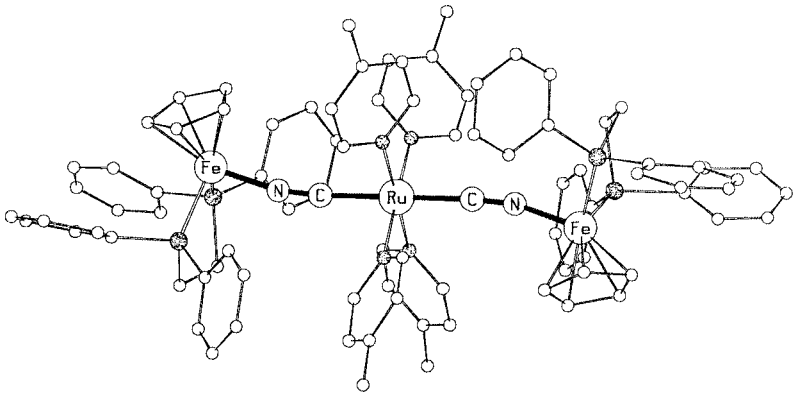

Figure 1. Molecular structure of the trinuclear cation of **2b**

would be facile[9] due to the *trans*-configuration of the central Ru^{II} ion.

The combination of $RuPy_4$ and FeCp(dppe) units confirmed this assumption. [$Ru(CN)_2Py_4$] complexes [Py = pyridine (**1a**), 4-methylpyridine (**1b**) or 4-ethylpyridine (**1c**)] were synthesized in which the variation of the pyridines provided a variation of the electron density at ruthenium. Their treatment with [FeCp(dppe)(CH_3CN)]Br yielded the trinuclear complexes [Cp(dppe)Fe−NC−$RuPy_4$−CN−Fe(dppe)Cp] $(PF_6)_2$ (**2a**−**c**) in a straightforward way. When crystallized with PF_6 counterions, **2a**−**c** are orange, air-stable, crystalline solids.

The identities of **2b** and **2c** were confirmed by crystal structure determinations. Figure 1 shows the structure of **2b** as a representative example. Table 1 lists the relevant bond lengths and angles.

Table 1. Relevant bond lengths (Å) and angles (°) in **2b** and **2c**

	2b	**2c**
Ru−N(Py)	2.086−2.120(7)	2.094−2.099(3)
Ru−C(CN)	2.061(9)	2.034(3)
C−N(CN)	1.16(1)	1.164(4)
Fe−N(CN)	1.911(7)	1.923−1.931(3)
Fe−P	2.185−2.195(3)	2.202−2.206(1)
N−Ru−N	89.2−90.3(3)	86.4−91.7(1)
C−Ru−N	88.0−90.8(3)	88.7−91.7(1)
C−Ru−C	178.3(5)	177.9(1)
Ru−C−N	175.2(7)	176.3−177.5(3)
Fe−N−C	166.6(7)	170.9−174.8(3)

The two structural units of complexes **1**, the $Ru(CN)_2Py_4$ unit and the Cp(dppe)Fe−NC unit, compare favorably with those in related complexes. Various $RuPy_4X_2$ complexes,[17] including $Ru(CN)_2Py_4$,[15] display the close to ideally octahedral coordination of ruthenium and the *trans* arrangement of the two ligands X. The isocyanide-ligated FeCp(dppe) unit is almost superimposable with that in dinuclear Cr−CN−Fe[18] and trinuclear Pt(CN-Fe)$_2$ complexes.[9] The electronic situation of complexes **2** is nicely reflected in the bond lengths and angles along the Ru−C−*N*−Fe arrays. The withdrawal of electron density from the cyanide ligand enhances the Ru→C π-backbonding, thereby making the Ru−C bonds rather short (cf. the Ru−N bonds). Likewise the lack of significant Fe→N π-backdonation results in Fe−N bond lengths that are significantly longer than the Fe−C bonds in related complexes with M−*N*−C−Fe arrays.[9,16,18] The various degrees of π-backdonation also explain a feature which is observed here like in most of our other M−C−*N*−M′ complexes: for the cyanide ligand the M−C−N angle (here Ru−C−N) is always close to 180°, while the M′−*N*−C angle (here Fe−*N*−C) shows significant bending, the average value of which in complexes **2** is 170°.

Redox Chemistry

The cyclic and square-wave voltammograms of **2a**−**c** show three waves in the oxidative range (see Figure 2 and Table 2). The first two of these are a closely spaced pair assignable to the FeCp(dppe) units.[9,18] The third one, at high voltage, belongs to the $RuPy_4$ unit. Characteristically the position of the Ru^{II}/Ru^{III} wave responds to the nature of the pyridine ligands, the more electron-rich of which in **2b** and **2c** facilitate the oxidation. The redox potentials for the FeCp(dppe) units are typically lower than that of Cp(dppe)Fe−CN (0.48 V), reflecting the more electron-rich state of iron due to the attachment of the cyanide's nitrogen.

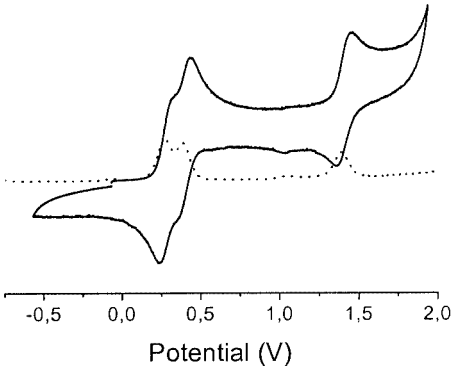

Figure 2. Cyclic (solid line) and square-wave voltammogram (dotted line) of **2b** (in CH_3CN, potentials vs. Ag/AgCl, scan rate 100 mV/s)

Table 2. Cyclovoltammetric data of complexes **2**[a]

	$E_{1/2}$ (1)	$E_{1/2}$ (2)	$E_{1/2}$ (3)
2a	0.29	0.40	1.52
2b	0.28	0.39	1.40
2c	0.27	0.38	1.40

[a] In CH_3CN, potentials (V) against Ag/AgCl, scan rate 100 mV/s.

The occurrence of two redox steps for the Cp(dppe)Fe units is the indicator of electronic communication between them. The potential separation of 110 mV is in the usual range.[9,12,13] Thus, complexes **2** are the third group of complexes synthesized by us for which a low-spin central unit with unfilled e_g orbitals enables electronic interactions between the two terminal redox-active organometallic units.

The potential separation is large enough to enable partial chemical oxidation of the FeCp(dppe) units. After treating **2a−c** with one equivalent of ferrocinium hexafluorophosphate in dichloromethane, the mixed-valent trinuclear complexes
$[Cp(dppe)Fe-NC-RuPy_4-CN-Fe(dppe)Cp](PF_6)_3$
(**3a−c**) could be isolated in good yields. Complexes **3** are only the second group of trinuclear complexes that have been isolated in the mixed-valent state. Prior to our work[9] the mixed-valent species could only be observed spectroscopically as transient species during redox titrations.

The identity of complexes **3** is evident from their analytical composition and from the fact that their voltammograms are identical to those of the corresponding complexes **2**. As before,[9] we failed to obtain crystals of a complex **3** suitable for X-ray analysis. Thus, the structural consequences of mixed valence in this type of complexes are still unknown. However, the spectroscopic data of **3a−c** (see below) clearly identify them as such.

Spectroscopy

The ν(CN) bands of complexes **1−3** (Table 3) provide good evidence for their structure and for their electronic situation. As expected, the symmetrical *trans*-configuration of the $Ru(CN)_2Py_4$ units in **1** and **2** gives rise to only one cyanide band in the IR spectra. Complexes **3**, with two distinctively different FeCp(dppe) units, show two widely separated ν(CN) absorptions.

Table 3. ν(CN) bands (in KBr, cm^{-1}) in the IR spectra

	1	**2**	**3**
a	2060	2071	2020, 2089
b	2055	2070	2014, 2090
c	2058	2070	2007, 2088

The ν(CN) band positions in complexes **2** are slightly raised relative to those in complexes **1**. As discussed by us several times before[9−13,16,18] this indicates that the kinematic effect (impediment of CN vibration due to the attachment of the second metal) is almost completely outbalanced by the π* effect (enhanced π-backdonation from ruthenium due to electron withdrawal by iron).

Complexes **3** provide a rare case of an internal reference for the size of these effects. The ν(CN) band position for the $Ru-C-N-Fe^{III}$ fragment is dramatically lowered because the Fe^{III} center is a much stronger electron acceptor than the Fe^{II} center. This induces a stronger π-backdonation from the Ru^{II} center into the CN-π* orbitals, causing a serious weakening of the C−N bond. We have observed this phenomenon in di- and trinuclear complexes before,[9,18] the most pronounced cases being the $L_nM-C-N-FeCl_3$ complexes with a ν(CN) band shift of −60 to −80 cm^{-1}.[19] The other ν(CN) band of complexes **3**, originating from the $Ru-C-N-Fe^{II}$ fragment, is now at significantly higher wavenumbers than in **1** or **2**. This is consistent with the opposite shift of the first band: there is less π-backdonation available on this side of the ruthenium atom, resulting in a lesser weakening of the C−N bond and hence a more pronounced appearance of the kinematic effect. Thus the IR spectra of complexes **1−3** are a demonstration of the classical *trans* effect observed in the IR spectra of octahedral metal carbonyls.

The absorptions in the electronic spectra of complexes **1−3** are listed in Table 4. Complexes **1** are yellow due to the tailing off of their strong absorption band in the near UV region. Complexes **2** are orange due to a weak absorption in the early visible range which results from the FeCp(dppe) units. Complexes **3** have deeper orange or brown colors which mostly results from an intensification of the latter absorption. This, in turn, results from the fact that the FeCp(dppe) absorption sits on the high-energy tail of a very broad medium-intensity absorption in the NIR. Figure 3 displays this for **3a**.

Table 4. Absorption bands [λ (ε·10^{-3})] in the visible and NIR spectra[a]

	1	**2**	**3**
a	374 (22.5)	368 (11.4), 540 (sh)	351 (19.0), 520 (sh), 980 (2.6)
b	369 (18.3)	376 (19.3), 560 (sh)	344 (17.3), 475 (1.7), 990 (2.8)
c	376 (24.1)	368 (23.1), 560 (sh)	342 (21.6), 475 (1.9), 970 (3.6)

[a] Dichloromethane solutions, λ in nm, ε in $M^{-1}cm^{-1}$.

The NIR absorption is a typical MMCT band, and it classifies complexes **3** as class II mixed-valent species according to Robin and Day.[20] We assign it as a long-range $Fe^{II} \rightarrow Fe^{III}$ electron transfer across the *trans*-$Ru(CN)_2$ center, in analogy to such transfers for *trans*-PtL_2-[9] and Fe(Pc)-centered[12] complexes. Alternatively, it might be considered a $Ru^{II} \rightarrow Fe^{III}$ electron transfer across a single cyanide bridge, in analogy to our observations for related $Fe(bpy)_2$-centered complexes.[21] This, however, is unlikely based on the redox potentials observed for the Ru and Fe units (cf. Table 2) and on our observations for short-range MMCT in complexes with similar redox properties.[10,12]

The MMCT bands observed here occur at higher energies than the ones observed by us before for PtL_2-[9] and

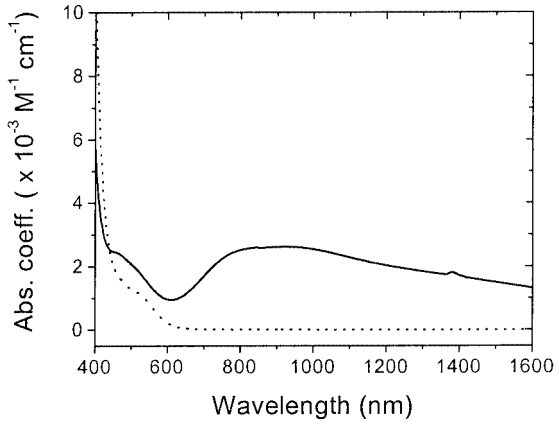

Figure 3. Electronic spectra of **2a** (dotted line) and **3a** (solid line) in dichloromethane

Fe(Pc)-centered[12] complexes with external FeCp(dppe) units. At first glance this might imply that the electronic interaction between the two iron centers is smaller than in the latter complexes. However, the quantitative treatment disproved this. It was done as before[9,12,18] by applying the Hush formalism for non-delocalized mixed-valent species according to Equation (1) and (2).[22]

$$H_{ab} = \tilde{\nu}_{max} a = 2.06 \cdot 10^{-2} (\tilde{\nu}_{max}/d)(\varepsilon_{max}\Delta\nu_{1/2}/\tilde{\nu}_{max})^{1/2} \quad (1)$$

$$a^2 = 4.24 \cdot 10^{-4} (\varepsilon_{max}\Delta\nu_{1/2}/\tilde{\nu}_{max} d^2) \quad (2)$$

For the computations $\tilde{\nu}_{max}$ was taken as 10000 cm^{-1} and $\Delta\nu_{1/2}$ as 6500 cm^{-1}, which is somewhat uncertain due to the large bandwidths of the MMCT bands. The value of d, the Fe−Fe distance, was taken from the structures of **2b** and **2c** as 10.2 Å. With these data the metal−metal interaction parameter, H_{ab}, is about 9000 cm^{-1} and the electron delocalization parameter a^2 about 0.8% for complexes **3**. Both these values are higher than the ones for the mixed-valent species with Fe^{II}−NC−Pt^{II}−CN−Fe^{III} backbones,[9] which indicates that the Fe···Ru···Fe system investigated here is a viable electronic conductor, as proposed in the introduction. In dinuclear species with M−CN−Fe(dppe)Cp arrays the electronic interaction between M and Fe, due to the 50% shorter distance, is naturally much stronger.[18,19]

Conclusions

This work has shown that Ru^{II} units with nitrogen ligands, which are famous as the external redox-active centers in classical mixed-valent dinuclear complexes,[23] are also favorable as the central units in trinuclear mixed-valent complexes. By a suitable choice of ligands on the three metal centers and by the suitable orientation of the bridging cyanide ligands it was ensured that a linear Fe−*N*−C−Ru−C−*N*−Fe array was obtained and that one-electron oxidations take place primarily at the iron centers. The basis for this is the inertness of octahedral Ru^{II}, which allows the unnatural orientation of the cyanide bridges (carbon attached to the electron-poor and nitrogen attached to the electron-rich metal) to persist.

These features have allowed, for the second time, the isolation of partially oxidized mixed-valent trinuclear complexes, i.e. the Fe^{II}−NC−Ru^{II}−CN−Fe^{III} species. Their spectroscopic investigation has identified their localized Fe^{II}/Fe^{III} nature and revealed a low-energy metal−metal charge transfer, which puts the complexes into class II of mixed-valent species according to the classification of Robin and Day. The electron delocalization parameter a^2 is of the order of 1%, which is considerably smaller than in related dinuclear complexes, but compares favorably with the values for other trinuclear complexes.

Among the trinuclear complexes of the type M-(μ-CN)-M′-(μ-CN)-M with organometallic units at the external positions only those with heavy and late transition metals at the center have allowed the detection of mixed valence by cyclic voltammetry and to investigate it by preparative redox chemistry, the prominent examples being those with Au^{I},[24] Pt^{II},[9] and Ru^{II} (this work). Their common feature is the low-spin electronic state with filled d_{xy}, d_{xz} and d_{yz} orbitals, i.e. those orbitals which provide π-interactions with the bridging cyanide ligands. This points to the π-bonding orbitals as the pathway for the metal−metal interactions. However, it is still too early to generalize this observation, and further studies, both preparative and theoretical, are necessary to gain a real understanding of these phenomena.

Experimental Section

For the general experimental and measuring techniques, see ref.[18] The starting materials $[RuCl_2(DMSO)_4]$,[25] $[Ru(CN)_2(pyridine)_4]$,[17] and $[FeCp(dppe)(CH_3CN)]Br$[26] were prepared as published.

1b: A mixture of $[RuCl_2(DMSO)_4]$ (300 mg, 0.62 mmol) and 10 mL of 4-methylpyridine was stirred at 100 °C for 30 min. After cooling to room temp. KCN (150 mg, 2.31 mmol) in 3 mL of water was added. After refluxing for 20 min all volatiles were removed in vacuo at 80 °C. The residue was extracted with 20 mL of dichloromethane. After filtration the extract was evaporated to dryness, leaving behind 230 mg (65%) of **1b** as a yellow powder, m.p. 280 °C (dec.). $C_{26}H_{28}N_6Ru \cdot 0.5CH_2Cl_2$ (525.62 + 42.46): calcd. C 56.03, H 5.15, N 14.79; found C 56.57, H 5.77, N 14.97.

1c: Prepared similarly to **1b** from $[RuCl_2(DMSO)_4]$ (300 mg, 0.62 mmol), 10 mL of 4-ethylpyridine and KCN (210 mg, 3.23 mmol). The dichloromethane extract was evaporated to 3 mL and chromatographed over a 10 × 1.5 cm silica gel column with CH_3CN/CH_2Cl_2 (1:4). A single yellow band was collected. Evaporation to dryness left behind 210 mg (51%) of **1c** as a yellow powder, m.p. 210 °C (dec.). $C_{30}H_{36}N_6Ru \cdot CH_2Cl_2$ (581.72 + 84.93): calcd. 55.85, H 5.75, N 12.61; found C 55.62, H 5.40, N 12.39.

2a: Complex **1a** (94 mg, 0.20 mmol) and $[FeCp(dppe)(CH_3CN)]Br$ (258 mg, 0.40 mmol) in 10 mL of dichloromethane were stirred for 8 h. NH_4PF_6 (68 mg, 0.42 mmol) was then added and the mixture stirred for a further 30 min. After filtration, slow diffusion of diethyl ether into the filtrate led, within one week, to the precipitation of 246 mg (63%) of **2a** as orange crystals, m.p. 180 °C (dec.).

Table 5. Crystallographic details

	2b·$2CH_2Cl_2$	**2c**·CH_3OH
Empirical formula	$C_{90}H_{90}Cl_4F_{12}Fe_2N_6P_6Ru$	$C_{93}H_{98}F_{12}Fe_2N_6OP_6Ru$
Molecular mass	2024.07	1942.36
Crystal size [mm]	0.2 × 0.1 × 0.1	0.6 × 0.3 × 0.3
Space group	*C*2/*c*	$P2_1/n$
Z	4	4
a (Å)	18.959(3)	19.865(5)
b (Å)	23.469(3)	22.317(6)
c (Å)	22.118(3)	21.351(6)
α (°)	90	90
β (°)	112.926(2)	96.209(5)
γ (°)	90	90
V (Å^3)	9064(2)	9410(4)
d(calcd.) (gcm^{-3})	1.48	1.37
μ(Mo-K_α) (mm^{-1})	0.78	0.64
hkl range	*h*: −23 to 23	*h*: −26 to 25
	k: −23 to 30	*k*: −31 to 23
	l: −29 to 15	*l*: −29 to 16
Measured reflections	23013	62769
Independent reflections	10546	25936
Observed refl. [$I > 2\sigma(I)$]	1680	15018
Parameters	546	1162
Refined reflections	10546	25936
R_1 (obsd.refl.)	0.070	0.051
wR_2 (all refl.)	0.208	0.164
Residual electron density [e/Å^3]	+1.7/-2.1	+1.0/-0.7

$C_{84}H_{78}F_{12}Fe_2N_6P_6Ru{\cdot}2CH_2Cl_2$ (1798.16 + 169.86): calcd. C 52.49, H 4.20, N 4.27; found C 52.52, H 4.32, N 4.36.

2b: Complex **1b** (114 mg, 0.20 mmol) and [FeCp(dppe)(CH_3CN)]Br (258 mg, 0.40 mmol) in 10 mL of methanol were stirred for 3 days. Addition of NH_4PF_6 (91 mg, 0.56 mmol) produced a red precipitate. This was filtered off and extracted with 6 mL of dichloromethane. After filtration the filtrate was layered with 1 mL of petroleum ether (60−70 °C) and 10 mL of diethyl ether. Within one week 273 mg (67%) of **2b** had precipitated as orange crystals, m.p. 255 °C (dec.). $C_{88}H_{86}F_{12}Fe_2N_6P_6Ru{\cdot}2CH_2Cl_2$ (1854.27 + 169.86): calcd. C 53.40, H 4.48, N 4.15; found C 53.65, H 4.66, N 4.12.

2c: Prepared similarly to **2b** from **1c** (67 mg, 0.10 mmol), [Cp(dppe)-Fe(CH_3CN)]Br (129 mg, 0.20 mmol) and NH_4PF_6 (34 mg, 0.21 mmol). Yield 80 mg (38%) of **2c** as orange crystals, m.p. 230 °C (dec.). $C_{92}H_{94}F_{12}Fe_2N_6P_6Ru{\cdot}2CH_2Cl_2$ (1910.38 + 169.86): calcd. C 54.27, H 4.75, N 4.04; found C 54.31, H 5.04, N 4.07.

3a: [Cp_2Fe]PF_6 (6.6 mg, 0.02 mmol) was added to a solution of **2a** (39 mg, 0.02 mmol) in 6 mL of dichloromethane. After stirring for 1 h the mixture was filtered and the filtrate layered with 10 mL of petroleum ether (60−70 °C). After 3 days 20 mg (51%) of **3a** had separated as brown crystals, m.p. 155 °C (dec.). $C_{84}H_{78}F_{18}Fe_2N_6P_7Ru$ (1943.13): calcd. C 51.92, H 4.05, N 4.32; found C 52.36, H 4.49, N 4.32.

3b: Prepared similarly to **3a** from **2b** (41 mg, 0.20 mmol). Yield: 30 mg (75%) of **3b** as orange crystals, m.p. 250 °C (dec.). $C_{88}H_{86}F_{18}Fe_2N_6P_7Ru$ (1999.23): calcd. 52.87, H 4.34, N 4.20; found C 52.86, H 4.60, N 4.22.

3c: Prepared similarly to **3a** from (42 mg, 0.20 mmol) of **2c**. Yield: 24 mg (58%) of **3c** as orange crystals, m.p. 220 °C (dec.). $C_{92}H_{94}F_{18}Fe_2N_6P_7Ru$ (2055.34): calcd. C 53.76, H 4.61, N 4.09; found C 53.05, H 4.81, N 3.99.

Structure Determinations:[27] Crystals of **2b** were obtained by layering a solution of **2b** in dichloromethane with hexane/diethyl ether, and those of **2c** by slow diffusion of diethyl ether into a solution of **2c** in methanol/dichloromethane. Diffraction data were recorded at −30 °C on a Bruker Smart CCD diffractometer and subjected to empirical absorption corrections. The structures were solved and refined with the SHELX program suite.[28] All hydrogen atoms were included with fixed distances and isotropic temperature factors 1.2-times those of their attached atoms. Parameters were refined against F^2. The *R* values are defined as $R_1 = \Sigma|F_o - F_c|/\Sigma F_o$ and $wR_2 = [\Sigma\{w(F_o^2 - F_c^2)^2\}/\Sigma\{w(F_o^2)^2\}]^{1/2}$. Drawings were produced with SCHAKAL.[29] Table 5 lists the crystallographic data.

Acknowledgments

This work was supported by the Deutsche Forschungsgemeinschaft (GK 307). We are indebted to Drs. W. Deck and H. Brombacher for help with the structure determinations.

[1] V. Balzani, A. Juris, M. Venturi, C. Campagna, S. Serroni, *Chem. Rev.* **1996**, *96*, 759−833.
[2] K. R. Dunbar, R. A. Heintz, *Prog. Inorg. Chem.* **1997**, *45*, 283−391.
[3] C. A. Bignozzi, J. R. Schoonover, F. Scandola, *Prog. Inorg. Chem.* **1997**, *44*, 1−95.
[4] H. Vahrenkamp, A. Geiß, G. N. Richardson, *J. Chem. Soc., Dalton Trans.* **1997**, 3643−3651.
[5] For references prior to 1997, see ref.[4]
[6] N. G. Connelly, G. R. Lewis, M. T. Moreno, A. G. Orpen, *J. Chem. Soc., Dalton Trans.* **1998**, 1905−1911.
[7] A. V. Macatangay, J. F. Endicott, *Inorg. Chem.* **2000**, *39*, 437−446.
[8] S. M. Kuang, P. E. Fanwick, R. A. Walton, *Inorg. Chem.* **2002**, *41*, 147−151.
[9] G. N. Richardson, U. Brand, H. Vahrenkamp, *Inorg. Chem.* **1999**, *38*, 3070−3079.

[10] A. Geiß, H. Vahrenkamp, *Eur. J. Inorg. Chem.* **1999**, 1793−1803.
[11] G. N. Richardson, H. Vahrenkamp, *J. Organomet. Chem.* **2000**, *593−594*, 44−48.
[12] A. Geiß, M. J. Kolm, C. Janiak, H. Vahrenkamp, *Inorg. Chem.* **2000**, *39*, 4037−4043.
[13] R. Appelt, H. Vahrenkamp, *Inorg. Chim. Acta* **2003**, *350*, 387−398.
[14] M.-L. Flay, H. Vahrenkamp, *Eur. J. Inorg. Chem.* **2003**, 1719−1726.
[15] B. J. Coe, T. J. Meyer, P. S. White, *Inorg. Chem.* **1995**, *34*, 3600−3609.
[16] T. Sheng, H. Vahrenkamp, *Inorg. Chim. Acta*, in print.
[17] B. J. Coe, T. J. Meyer, P. S. White, *Inorg. Chem.* **1995**, *34*, 593−602.
[18] N. Zhu, H. Vahrenkamp, *Chem. Ber./Recueil* **1997**, *130*, 1241−1252.
[19] T. Sheng, H. Vahrenkamp, *J. Argentine Chem. Soc.*, in print.
[20] M. B. Robin, P. Day, *Adv. Inorg. Chem. Radiochem.* **1967**, *10*, 247−422.
[21] N. Zhu, H. Vahrenkamp, *J. Organomet. Chem.* **1998**, *573*, 67−72.
[22] N. S. Hush, *Prog. Inorg. Chem.* **1967**, *8*, 391−444.
[23] C. Creutz, *Prog. Inorg. Chem.* **1983**, *30*, 1−73.
[24] N. C. Brown, G. B. Carpenter, N. G. Connelly, J. G. Crossley, A. Martin, A. G. Orpen, A. L. Rieger, P. H. Rieger, G. H. Worth, *J. Chem. Soc., Dalton Trans.* **1996**, 3977−3984.
[25] I. P. Evans, A. Spencer, G. Wilkinson, *J. Chem. Soc., Dalton Trans.* **1973**, 204−209.
[26] P. M. Treichel, D. C. Molzahn, *Synth. React. Inorg. Met.-Org. Chem.* **1979**, *9*, 21−29.
[27] CCDC-219798 (for **2b**) and -219799 (for **2c**) contain the supplementary crystallographic data for this paper. These data can be obtained free of charge at www.ccdc.cam.ac.uk/conts/retrieving.html [or from the Cambridge Crystallographic Data Center, 12, Union Road, Cambridge CB2 1EZ, UK; Fax: (internat.) +44-1223/336-033; E-mail: deposit@ccdc.cam.ac.uk].
[28] *SHELX* program package for the Bruker Smart CCD diffractometer, version 5.1, **2002**.
[29] E. Keller, *SCHAKAL for Windows*, Universität Freiburg, **2001**.
Received September 19, 2003
Early View Article
Published Online February 16, 2004

